

Photoluminescence and photoconductivity in lanthanide doped chemically deposited CdS-Se films

R. S. SINGH

Govt. College Utai, Durg – 491107, Chhattisgarh, India

Some interesting results of photoluminescence (PL) and photoconductivity (PC) observed in chemically deposited films of lanthanide doped CdS-Se are presented in this talk. Strong PL and high photosensitization are observed at particular concentrations of the two bases. An edge emission corresponding to radiative decay of the free exciton and a broad green emission related to exciton-donor complexes formed in presence of S / excess Cd are observed in the PL emission spectra of various CdS-Se films. In doped films, characteristic emissions of lanthanides such as Ho and Sm are observed. Some properties related to nanocrystalline effects are also found. Results of optical absorption spectra also support such observations i.e. apart from host absorption, absorption due to impurities are observed. High photosensitization has also been observed under some special conditions. Results of XRD confirm the presence of CdS and CdSe. SEM studies show growth of layered structure.

(Received July 5, 2009; accepted November 12, 2009)

Keywords: CdS-Se, Thin films, Photoluminescence, RE doping, XRD, SEM

1. Introduction

The wide technological applications of CdS type materials make the PL and PC studies important. Some of the important applications of PL are lamp phosphors and display devices and those of PC are xerography and IR detectors etc. PL edge emission was extensively studied in CdS by several workers [1-3] and was related to excitonic transitions involving donor/acceptor-exciton complexes [4]. Similarly PC of CdS and CdSe were extensively studied by Bube and co-workers [5,6]. The effect of alloying of CdS, CdSe and other II-VI group compounds on the PL and PC properties has attracted the interest of research workers in recent years. Regarding the PL spectral studies of CdS-Se, Shevel et al [7] studied the localized electronic states created by the compositional disorder in CdS-Se employing the pico-second luminescence spectral studies. Pagliara et al [8] correlated the structural disorders in $\text{CdS}_x\text{Se}_{1-x}$ to localization of excitons observed in PL spectra. Regarding PC studies Gupta et al [9] reported PC studies in $\text{CdS}_x\text{Se}_{1-x}$ evaporated layers and used grain-boundary-trapping model to determine the barrier height at the inter-crystalline boundary. Further, application of high speed chemically deposited $\text{CdS}_{0.20}\text{Se}_{0.80}$ photoconductor as line image sensors and superior stability were reported by Yukami et al [10] and Rincon et al [11] respectively. Encouraged with such results, CdS-Se was selected as the base material for the present studies. Bhushan and coworkers [12-15] found enhancement in PL and PC due to doping of lanthanides in (Cd-Zn)S and (Cd-Pb)S. So for the present work Ho and Sm were selected as impurities. While Ho can be expected to sensitize PL due to its well separated energy levels, it can also help in PC due to valence electrons. Inorganic compounds using Ho as impurity have got important applications in luminescent

devices like luminescent lamps, cathode ray tubes and lasers [16]. Further, reason for selecting Sm has been the energy levels of its emitting state $^4\text{G}_{5/2}$ lying below the energy level of the trap states in Cd(S-Se) base, hence energy transfer from host defects to rare earth activator Sm^{3+} could occur [17] and hence presented interesting activator.

The present paper reports results of PL emission spectra, PC rise and decay, absorption spectra, XRD and SEM studies of chemically deposited films of Ho and Sm doped CdS-Se.

2. Experimental details

The films were prepared by dipping microscopic glass slides of dimension 24 x 75 mm in a mixture of 1 M solution of cadmium acetate, thiourea, tri-ethanolamine, 0.01 M solutions of cadmium chloride, holmium oxide / samarium nitrate and 0.42 M solution of sodium selenosulphate in appropriate proportions in presence of 30% aqueous ammonia. Being insoluble in water, solution of holmium oxide was prepared in sulphuric acid; solutions of all other chemicals were prepared in double distilled water. The pH value of the mixture was ~ 9. After deposition the films were sprayed with distilled water to wash out the uneven overgrowth of grains at the surface and dried in open atmosphere at room temperature (RT). The thickness of the films was measured by multiple beam interference method and was found to lie in the range 0.1 to 0.9 μm .

For PC measurements coplanar colloidal silver paint electrodes of 1.5 mm width and 24 mm length were formed at a separation of 2 mm. The PL cell consisted of films deposited on the substrates. An incandescent bulb of 100 W was used as excitation source for PC growth and decay studies. The PL excitation source was a high

pressure Hg source from which 365 nm radiation was selected by using Carl Zeiss interference filter. An RCA-6217 photomultiplier tube operated by a highly regulated power supply was used for detection of PL light emission. The integrated light output in the form of current was recorded by a sensitive polyflex galvanometer (10^{-9} A/mm). A prism monochromator was used for PL emission spectral studies. The absorption spectra were recorded with the help of Shimadzu Pharmaspec-1700 spectrophotometer. XRD and SEM studies were performed at IUC-DAE, Indore using models Rigaku RU:H2R horizontal Rotaflex and JEOL-JSM 5600 respectively.

3. Results and discussions

3.1 SEM Studies

The SEM micrographs of $\text{CdS}_{0.70}\text{Se}_{0.30}$ and $\text{CdS}_{0.95}\text{Se}_{0.05}$ films are shown in fig. 1 and 2 respectively. These configurations correspond to maximum PL and PC response respectively. A leafy structure is observed in both the figures which may appear due to layered growth of the films. The thickness of the layers lie in the nano-range. A similar nature along with some micro-crystallites spread over the leafy structure are found in doped films.

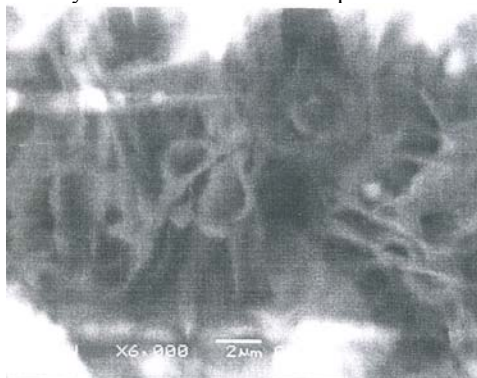


Fig. 1. SEM micrograph of $\text{CdS}_{0.95}\text{Se}_{0.05}$ film.



Fig. 2. SEM micrograph of $\text{CdS}_{0.70}\text{Se}_{0.30}$ film

3.2 XRD Studies

Fig. 3 shows the X-ray diffractogram of $\text{CdS}_{0.95}\text{Se}_{0.05}$ film. The assignment of peaks have been made by using JCPDS data and comparing the evaluated values of lattice constants with those of the reported values. Thus, prominent peaks of CdS and CdSe are observed.

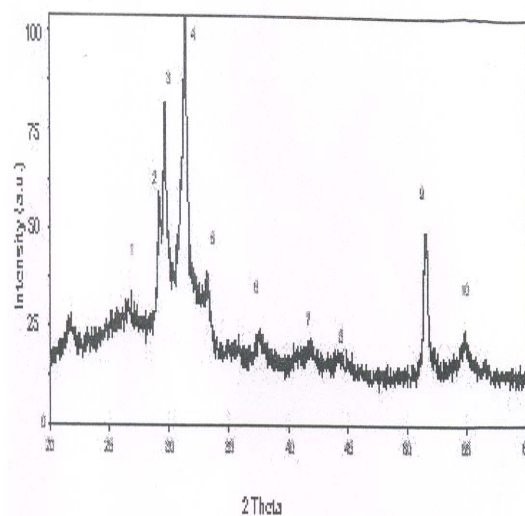


Fig. 3. X-ray diffractogram of $\text{CdS}_{0.95}\text{Se}_{0.05}$ film peak 1: $(111)_c\text{CdS}$, 2: $(101)_h\text{CdS}$, 3: $(101)_h\text{CdSe}$, 4: $(200)_c\text{CdS}$, 5: $(102)_h\text{CdSe}$, 6: $(102)_h\text{CdS}$, 7: $(110)_h\text{CdSe}$, 8: $(220)_c\text{CdS}$, 9: $(311)_c\text{CdS}$, 10: $(222)_c\text{CdS}$.

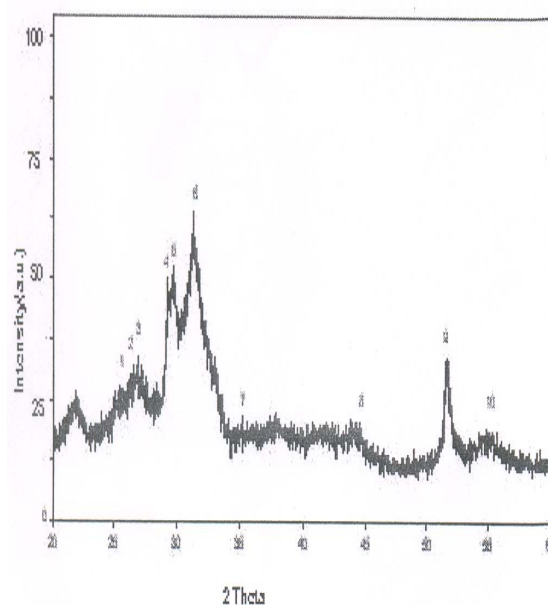


Fig. 4. X-ray diffractogram of $\text{CdS}_{0.95}\text{Se}_{0.05}\text{CdCl}_2\text{Ho}$ film; peak 1: $(002)_h\text{CdSe}$, 2: $(111)_c\text{CdS}$, 3: $(002)_h\text{CdS}$ or $(101)_h\text{CdCl}_2$, 4: $(222)_c\text{Ho}_2\text{O}_3$, 5: $(101)_h\text{CdS}$, 6: $(200)_c\text{CdS}$, 7: $(102)_h\text{CdSe}$, 8: $(220)_c\text{CdS}$, 9: $(311)_c\text{CdS}$, 10: $(222)_c\text{CdS}$

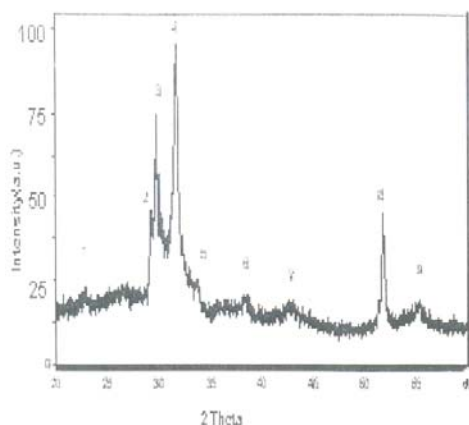


Fig.5. X-ray diffractogram of $CdS_{0.70}Se_{0.30}:CdCl_2, Ho$ film; peak 1: $(100)_h CdSe$, 2: $(101)_h CdSe$, 3: $(101)_h CdS$, 4: $(200)_c CdS$, 5: $(102)_h CdSe$ or $(400)_c H_2O_3$, 6: $(102)_h CdS$, 7: $(110)_h CdSe$, 8: $(311)_c CdS$, 9: $(222)_c CdS$.

The X-ray diffractograms of $CdS_{0.95}Se_{0.05}:CdCl_2, Ho$ and $CdS_{0.70}Se_{0.30}:CdCl_2, Ho$ films are shown in fig. 4 and 5 respectively. From these diagrams along with prominent peaks of CdS and CdSe, some lines of $CdCl_2$ and Ho are also seen. The X-ray diffractograms of Sm doped films are shown in fig. 6 and 7 and in both some lines of Sm are also assigned.

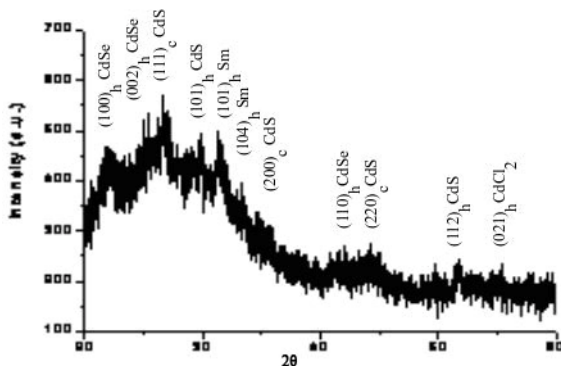


Fig. 6. X-ray diffractogram of unannealed $Cd(S_{0.95}Se_{0.05}):CdCl_2(3 ml), Sm(3 ml)$ film

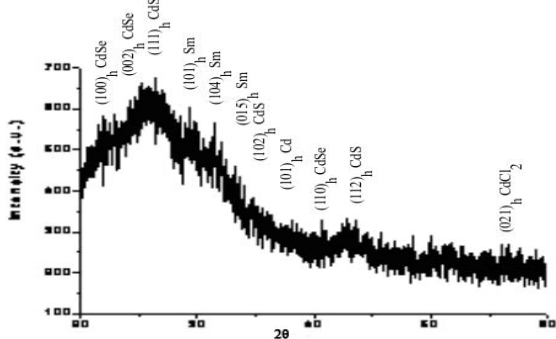


Fig. 7. X-ray diffractogram of unannealed $Cd(S_{0.7}Se_{0.3}):CdCl_2(2 ml), Sm(2 ml)$ film

Different layers of CdS are observed in cubic as well as hexagonal phases. Such layers are known to be created through different arrangements of atomic layers. The hexagonal and cubic phases consist of sequence of atomic layers defined as ABABAB--- and that of cubic as ABCABCABC—[18]. It is also possible to find mixed forms with random stacking of very long period repeats as is found in polytypes of SiC [19]. The total crystal consists of different atomic layers of CdSe in hexagonal phases. According to Langer et al [20], one might think of solid solutions as mixtures of microcrystalline regions of pure CdSe and CdS, where each microregion might consist of a number of unit cells of each material. Such a model can explain uniform shift of absorption edge with variation in composition. A possibility of solid solution consisting of statistical distribution of CdSe and CdS with respect to their overall concentration was also mentioned by these workers. It is worth noting that shift of absorption edge has been observed in the present case.

3.3 Absorption spectral studies

Fig. 8 shows optical absorption spectra of different CdS-Se films. The films prepared with different mole % of S and Se show variation in the band gap over different compositional range (e.g. CdS : 2.42 eV; $CdS_{0.40}Se_{0.60}$: 2.13 eV) indicating the formation of a common lattice of CdS-Se through solid solutions. Curves 1 and 2 represent the optical absorption spectra of $CdS_{0.95}Se_{0.05}$ and $CdS_{0.70}Se_{0.30}$ films respectively. A steep increase in the absorption corresponding to the onset of band-to band transition is observed in both the curves. Further, the optical absorbance decreases in presence of impurity as is shown for Ho doped films in curves 3 and 4 respectively. The curves of doped films are flat and extended in impurity doped films showing incorporation of more energy levels in the band gap due to impurities. With increasing concentration of Se magnitude and width of absorption decreases. A narrower and resolved absorption peak correspond to narrower size distribution. A blue shift in absorption edges and the energies

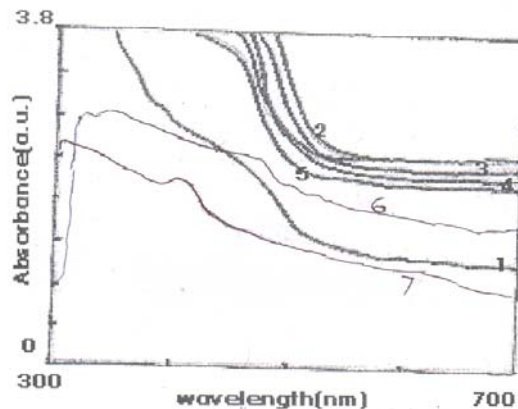


Fig. 8. Absorption spectra of different CdS-Se films 1: $CdS_{0.95}Se_{0.05}$; 2: $CdS_{0.7}Se_{0.30}$; 3: $CdS_{0.95}Se_{0.05}:CdCl_2, Ho$; 4: $CdS_{0.70}Se_{0.30}:CdCl_2, Ho$; 5: $CdS_{0.95}Se_{0.05}:CdCl_2, Ho$ (90% aq. ammonia); 6: $CdS_{0.70}Se_{0.30}:CdCl_2, Ho$ (90% aq. ammonia); 7: $CdS_{0.95}Se_{0.05}:CdCl_2, Sm$.

corresponding to the onset of direct band-to-band transition in Ho doped films prepared with 90% aqueous ammonia (curves 5 and 6) compared to those of films prepared with 30% aqueous ammonia suggests a decrease in particle size. It is known that in nanocrystalline materials the energy spectrum is quantized and the highest occupied valence band and lowest unoccupied conduction band are shifted to more positive and negative values resulting in a blue shift in absorption edge onset of direct absorption. The optical absorption of Ho doped films a hump is observed in 425-525 nm region corresponding to absorption related to transition $^5I_7 \rightarrow ^5F_3$ in Ho [21]. Similarly in Sm doped films a hump at around 404 nm (curve 7) corresponds to $^6H_{5/2} \rightarrow ^4K_{11/2}$ transition in Sm^{3+} [22].

3.4 PL emission spectra

Fig. 9 shows PL emission spectra of CdS and CdS-Se films at different compositions of S and Se. The emission spectrum of CdS shows a peak at 515 nm and those of CdS-Se films show two peaks. The emission peak at 515 nm of CdS corresponds to band gap 2.42 eV and so it can be assumed to be the edge emission of CdS. Thomas and Hopfield [23] attributed the edge emission to transitions associated with donor / acceptor exciton complexes. Jeong and Yu [24] observed the excitonic effects in CdS at RT. Thus, in present cases also the edge emission can be attributed to excitonic transitions. The PL emission in CdS-Se is significantly broader than pure CdS and CdSe due to excitonic effects [25, 26]. In the present studies, two broad peaks are observed in CdS-Se. The peak observed at ~ 525 nm shows a shift towards higher wavelengths with increasing mole % of Se corresponding to reduction in band gap. So, this emission can be identified as edge emission of CdS-Se. Due to similar excitonic nature of emissions in both CdS and CdSe this emission can be attributed to radiative decay of free exciton. The position of broad band at 503 nm remains unchanged and may be attributed to excitons bound to neutral donor levels formed by sulphur / excess Cd. In present method, excess Cd was produced as was confirmed by EDX studies whereas sulphur was produced in solid phase by thiourea and sodium thiosulphate both which can be substituted in the lattice. For increasing concentration of Se, higher volumes of sodium selenosulphate were added resulting in formation of more sulphur thus enhancing the emission in its presence. In Ho doped films, emissions observed at 495 nm and 545 nm are related to transitions $^5F_3 \rightarrow ^5I_8$ and $^5S_2 \rightarrow ^5I_8$ [21]. Similarly, in Sm doped films emissions corresponding to transitions $^4G_{5/2} \rightarrow ^6H_{5/2}$, $^4G_{5/2} \rightarrow ^6H_{7/2}$ and $^4G_{5/2} \rightarrow ^6H_{9/2}$ giving emissions at 563, 595 and 614 nm [22].

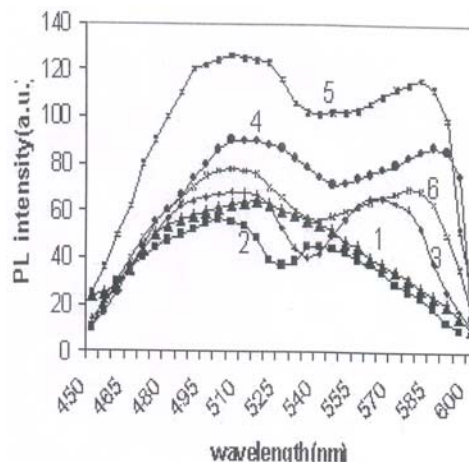


Fig. 9. PL emission spectra of CdS and different CdS-Se films: 1. CdS, 2. CdS_{0.95}-Se_{0.05} 3. CdS_{0.90}-Se_{0.10} 4. CdS_{0.80}-Se_{0.20} 5. CdS_{0.70}-Se_{0.30} 6. CdS_{0.60}-Se_{0.40}

3.5 PC studies

The PC growth and decay curves for different CdS-Se films are shown in fig. 10. In all such curves, a rapid rise in photocurrent results due to generation of carriers. After this initial rise, when recombination starts becoming effective, the rate of rise becomes slower and finally a balance between the two effects make the current saturated. The decay curves consist of initially a fast decrease followed by a slow decrease. While fast decrease is related to direct recombination effects and the slow decrease is related to release of trapped electrons from deep traps formed in CdS-Se. Parameters like life-time, mobility and trap depths were obtained by methods published elsewhere [12] and are listed in table-1. From these values it is inferred that high photosensitization in such materials is observed due to increase in lifetime, mobility and carrier concentration.

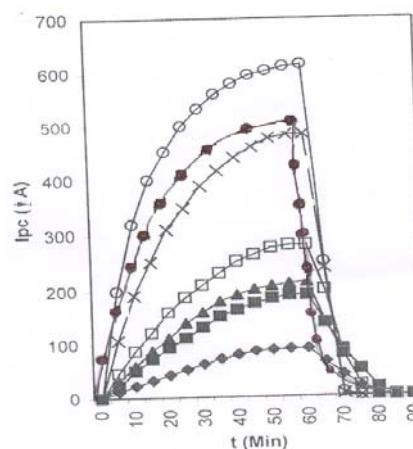


Fig.10. PC rise and decay curves for different CdS-Se films: ● CdS ; ■ Cd(S_{0.95}-Se_{0.05}) ; Cd(S_{0.95}-Se_{0.05}):CdCl₂; □ Cd(S_{0.95}-Se_{0.05}): CdCl₂; □ Cd(S_{0.95}-Se_{0.05}): CdCl₂; ● Cd(S_{0.95}-Se_{0.05}):CdCl₂, Sm ; o Cd(S_{0.95}-Se_{0.05}):CdCl₂, Ho.

4. Conclusions

The chemically deposited CdS-Se films show layered growth morphology in the SEM studies. In XRD studies, existence of CdS, CdSe, CdCl₂ and impurities are found. PL emission of such films show two peaks in absence of impurities. Presence of impurities are found in terms of transitions in these elements. Absorption studies also support their existence. Such studies also show reduction in band gap due to increasing concentrations of CdSe. At a particular concentration, higher values of photosensitizations are also observed.

Acknowledgements

The author is grateful to IUC-DAE, Indore (M.P.) for SEM and XRD.

References

- [1] R. E. Halsted, M. Aven, Phys. Rev. Lett. **14**, Y533(2-1) (1965).
- [2] S. Iida, M. Toyama, J. Phys. Soc. (Japan) **31**, 190 (1971).
- [3] Y. Kokubun, T. Kaeriyama, J. Appl. Phys. (Japan) **14**, 1403 (1975).
- [4] D. G. Thomas, J. J. Hopfield, Phys. Rev. **128**, 2135 (1962).
- [5] S. M. Thomsen, R. H. Bube, Rev. Sci. Instrum., **26**, 664 (1955).
- [6] R. H. Bube, Phys. Rev. **99**, 1105 (1955).
- [7] S. Shevel, R. Fischer, G. Noll, E. O. Gobel, P. Thomas, C. Klingshirn, J. Lum. **37**, 45 (1987).
- [8] S. Pagliara, L. Sangaletti, L. E. Depero, V. Capozzi, G. Perna, Appl. Surf. Sci. **186**, 527 (2002).
- [9] P. Gupta, S. Choudhary, A. K. Pal, J. Phys. D. Appl. Phys. **26**, 1709 (1993).
- [10] N. Yukami, M. Ikeda, Y. Harada, M. Nishikura, T. Nishikura, Electronic Devices (IEEE) **33**, 520 (1986).
- [11] M. E. Rincon, M. Sanchez, R. Garcia, J. Electrochem. Soc. **145**, 3535 (1998).
- [12] S. Bhushan, M. Mukherjee, P. Bose, Rad. Effect and Defects in Solids **153**, 367 (2001).
- [13] M. Mukherjee, S. Bhushan, Opt. Mater. **22**, 51 (2003).
- [14] T. Chandra, S. Bhushan, J. Mater. Sci. **39**, 6303 (2004).
- [15] S. Bhushan, S. Shrivastava, Opt. Mater. **28**, 1334 (2006).
- [16] P. Dorenbos, J. Lum. **91**, 91-106 (2000).
- [17] K.L. Frindel, M.H. Bartl, M.R. Robinson, G.C. Bazan, A. Popitsch, G.D. Stucky, J. Solid State Chem. **172**, 81 (2003).
- [18] C. Kittel, Introduction to Solid State Physics (7th edition) (John Wiley & Sons) p.18, (1995).
- [19] Ibach Herald, Lüth Hans, Solid State Physics (An Introduction to Theory and Expt.) (Springer International Student Edn.) p.25 (1991).
- [20] D.W. Langer, Y.S. Park, R.N. Euwama, Phys. Rev. **152**, 788 (1966).
- [21] T. Ishizaka, Y. Kurokawa, J. Lum. **92**, 56-63 (2001).
- [22] Li Yu-Chun, Chang Yen-Hwei, Lin Yu-Feng, Chang Yee-Shin & Lin Yi-Jing, J. Alloys and Compounds **439**, 367 (2007).
- [23] D.G. Thomas, J.J. Hopfield, Phys. Rev. **128**, 2135 (1962).
- [24] T.S. Jeong, P.Y. Yu, J. Phys. Soc. (Korea) **36**, 102 (2000).
- [25] S. Shevel, R. Fischer, G. Noll, E. O. Gobel, P. Thomas, C. Klingshirn, J. Lum. **37**, 45 (1987).
- [26] R. S. Singh & S. Bhushan, Chalcogenide Letters **5**(12), 377 (2008). "Photoconductivity and Photoluminescence Studies of chemically deposited Cd(S-Se):CdCl₂, Dy films".

Corresponding author: rss.bhilai@gmail.com